Infinite-NTU Modeling for Studying Charging Cycle of Packed-Bed Solar Thermal Energy Storage

Yacob G. Hiben[1*]

[1]Thermal and Energy Systems Chair, School of Mechanical and Industrial Engineering, Mekelle University, Endayesus Campus, Mekelle, Ethiopia

[*]yacob.gebreyohannes@mu.edu.et

Abstract

Thermal Energy Storage (TES) is a key component for solar thermal applications to bridge the gap between the demand for thermal energy and the supply of solar energy, whose availability depends on the time of day and season. Thus, cost-effective packed-bed thermal containers filled with a solid storage medium have been proposed for high-temperature sensible heat storage as materials are abundant and relatively cheap. Thus, it is necessary to investigate their performance and temperature profiles during the charge-discharge cycle. Several models are available for this purpose. Typically, the more detailed a model, the greater the computational effort required to solve it, and hence a time-efficient model is needed to prevent excessively long computation times for long-term analysis. At the more basic level, the common Hughes E-NTU model and the less realistic simplified Infinite-NTU model are very important for their less time and computational effort. In this paper, the appropriateness of employing the Infinite-NTU model was evaluated to investigate the performance of a typical and scalable rock-bed TES as a case study. The results presented provide a methodology to quickly test the validity of the model and predict the temperature profile for the case under study. Accordingly, such simple charge-discharge cycle thermal performance predictions are important to plan, design, and rapidly deploy a reliable and economical solar thermal system for the supply of valuable heat to high-temperature demanding applications of power generation and industrial processes as part of a rapid shift towards non-polluting renewable energy.

Keywords: Solar Thermal, TES, Packed-bed, NTU model, Temperature profile

1. Introduction

Basic configurations of solar thermal systems consist of solar thermal collectors, heat transfer fluid, interconnecting pipes, pumps, heat exchangers, and thermal storage and/or auxiliary backup. Storage of solar heat allows buffering mismatches between the heat demand and the availability of the intermittent supply of solar resources. Due to its continuous high-temperature demand, thermal energy storage (TES) is a key component for high-temperature solar thermal applications such as concentrating solar power plants (CSP) and energy-intensive industrial processes. The decision for thermal storage installation depends on the cost/benefit ratio as well as on the control and stagnation concept of a solar system.

TES has a high energy storage density on average up to 10, 000 kW for about 6 hours (Global Energy Systems Program, 2020). TES systems are classified as sensible heat storage, latent heat storage, and thermochemical storage (Kuravi et al., 2013). Traditional and current plants have employed sensible heat systems to store their excess energy. In sensible heat storage, the heat energy is stored as internal energy depending on temperature changes in the storage material. In this scenario, a media (solid or liquid) may store energy by raising its temperature in line with its heat capacity. Among the types of sensible heat storage, hot water (<100 ^{0}C) and pressurized water systems (>100 ^{0}C) are considered the most common commercial technology, due to the cost, simplicity, and high specific heat of water relative to a majority of other storage media (Furbo, 2015; Kulkarni et al., 2008). The costs of unpressurized hot water storage range on the order of thousands of dollars depending on size, with a 0.5 m^3 tank costing roughly $1300 and a 200 m^3 tank $60,000 (USD in 2002), while costs of pressurized systems are generally higher (Wallerand et al., 2018; Heliodyne. Inc, n.d.).

Although molten salt TES is well-known as the commercial state of the art for high-temperature applications, it is fairly expensive and therefore cost-effective systems are desirable (Kolb et al., 2012). Currently, molten salt two-tank systems limited by operational temperatures (< 600°C) and high costs (> $35/kWht) are employed. To reduce costs and operate at higher temperatures, two other options have been investigated by (Jacob et al., 2017): a packed bed of rocks and a packed bed of encapsulated phase change material (EPCM). Both of these options have the potential to replace the current two-tank molten salt systems and provide low-cost future storage options.

doi:10.18086/solar.2021.01.10 Available at http://proceedings.ises.org

Packed-bed thermal reservoirs filled with a solid storage medium such as gravel or pebbles are key options for sensible heat storage technologies, as materials are abundant and relatively cheap (McTigue et al., 2018). Packed-beds incorporating air as the heat transfer fluid have been suggested as a more cost-effective approach due to the low-cost of rock and ample availability of air (Zanganeh et al., 2012). Concrete and cast ceramics have also been studied as sensible heat thermal storage materials due to their low-costs, good thermal conductivities, and moderate specific heat capacity. In concrete TES, the high thermal conductivity enhances the heat transfer dynamics in the system and high heat capacity is desirable since it reduces the storage volume. Composite materials such as fiberglass reinforced epoxy concretes have specific heat values close to 1 kJ/kg K (Zhang et al., 2016; Hoivik et al., 2017).

Direct cost estimates of several TES systems were investigated by (Jacob et al., 2017). This comprises the cost of the tank, filler material(s) and heat transfer fluid (HTF), encapsulation (if required), instrumentation and control, and the piping (ductwork) and valves. The investigated systems include traditional two-tank molten salt system (2-Tank), EPCM system utilizing one PCM (1EPCM), cascaded EPCM system utilizing 2 PCMs (2EPCM), quartz/rock thermocline system (ThermoQS), and thermocline system utilizing a geopolymer (ThermoG). The costs of these systems were estimated over a range of temperature differences (ΔT=100-500°C) and a variety of HTFs (molten salt and air). The results of this are presented in Figure 1.

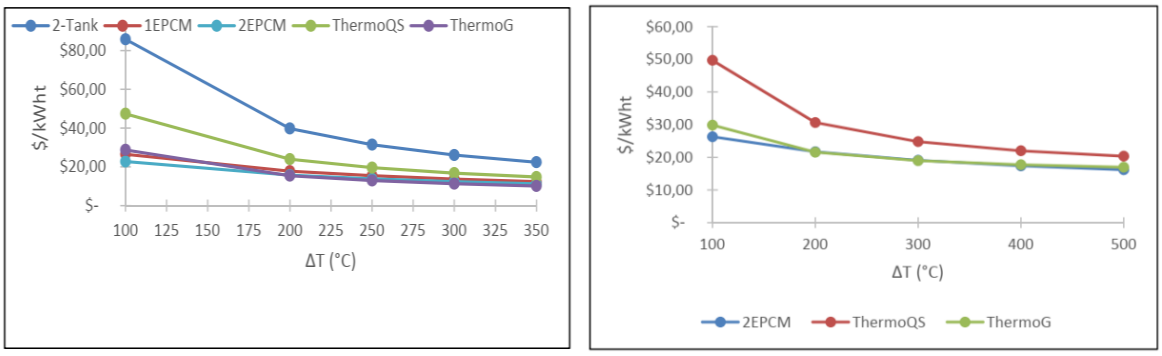

(a) (b)

Fig. 1: Comparison of TES costs with (a) Molten Salt HTF, (b) Air HTF

Figure 1(a) shows that all the systems investigated resulted in a lower cost than the traditional two-tank molten salt system for all temperature differences. It can also be seen that for a ΔT of 300°C, the EPCM systems, thermocline system with quartz/rocks, and the thermocline with geopolymer results in 50%, 35%, and 60% savings, respectively. As expected the cascaded system resulted in lower cost estimates than the one PCM system for all temperature differences. Figure 1(b) shows a comparison between the systems with air as the HTF. Initially the cascaded system results in a lower cost but is more expensive when ΔT > 200°C. The thermocline system with quartz/rocks are approximately the same prices as the cascaded EPCM system when ΔT > 300°C. For all temperature differences the geopolymer thermocline system resulted in a lower cost than the quartz/rock system due to the higher heat capacity of the geopolymer filler.

To evaluate the viability of rock-bed TES systems, it is necessary to study their charge-discharge thermal performance and the associated effect on power generation. Essentially, this requires the ability to predict the rock and air temperature profiles through the bed during a charge-discharge cycle. Different models are available for this purpose, including, the more detailed models such as the “Continuous Solid Phase” model whose governing equations account for thermal conduction through the rock and air (Wakao et al., 1979). Usually, the more detailed models require greater computational effort to be solved. This is infrequently problematic for the simulation of a few charge-discharge cycles; however, for long-term analysis such as in the context of annual CSP plant performance simulation, a time-efficient model is needed to avoid excessively long computation times. This is particularly the case when conducting plant-level theoretical design or optimization studies. There are also models at the more basic level such as the popular Hughes E-NTU (Effectiveness – Number of Transfer Units) model and the simplified Infinite-NTU model (Hughes et al., 1976; Duffie, 2013). Unlike the E-NTU model, the Infinite-NTU model assumes an infinite heat transfer coefficient between the solid bed and heat transfer fluid, which implies comparable solid bed and heat transfer fluid temperature profiles.

This paper, therefore, evaluates the accuracy and computational efficiency of the Infinite-NTU model when simulating the performance of a typical and scalable rock-bed TES system as a case study. Based on its

appropriateness, the Infinite-NTU model is employed for the simulation and evaluation of the rock-bed TES system with the given parameters and characteristics. For every hour of operation over charge cycles, the heat transfer fluid (air) and rock-bed temperature profile predictions were achieved for the ten segments of the storage system considered. Thus, such simple charge-discharge cycle thermal performance predictions are found important to quickly plan and design a reliable and economical TES system for a rapid shift towards non-polluting renewable energy systems.

2. Materials and Methods

2.1. Basic Theory

The assumptions underlying the E-NTU model are those of the Schumann model (Schumann, 1929). Flow is assumed to be one dimensional with a uniform axial flow speed, there is no thermal loss from the bed walls, radiant and conductive heat transfer through the bed is negligible, the internal thermal resistance of each solid particle (rock) can be neglected, and the thermal capacitance term of the air can be neglected. These assumptions give rise to the Schumann equations summarized in Table 1.

Tab. 1: The Schumann equations for the fluid and solid phases

The Schumann Equations	Remark
$\frac{\partial T_f}{\partial z} = \frac{h_v A_{cs}}{\dot{m} C_{pf}}(T_s - T_f)$ $h_v = 650\left(\frac{G_f}{D}\right)^{0.7}$ $G_f = V_f \rho_f$ $NTU = \frac{h_v A_{cs} L}{\dot{m} C_{pf}} = \frac{h_v L}{G_f C_{pf}}$ $\frac{\partial T_f}{\partial z} = \frac{NTU}{L}(T_s - T_f)$ $\frac{\partial T_s}{\partial t} = \frac{h_v}{(1-\varepsilon)\rho_s C_s}(T_f - T_s)$ $\tau = \frac{\rho_s (1-\varepsilon) A_{cs} L C_s}{\dot{m} C_{pf}}$ $\frac{\partial T_s}{\partial t} = \frac{NTU}{\tau}(T_f - T_s)$	T_f – Fluid Temperature (air) [^{0}C or K] z – Axial coordinate in the flow direction [m] h_v – Volumetric heat transfer coefficient [W/m^3-K] A_{cs} – Cross-section area [m^2] m – Mass flow rate [kg/s] C_{pf} – Fluid isobaric specific heat capacity (air) [J/kg-K] T_S – Solid Temperature (rock) [^{0}C or K] h_v – Volumetric heat transfer coefficient [W/m^3-K] G_f – Fluid mass flux/velocity (air) [kg/s-m^2] D – Equivalent particle diameter [m] V_f – Fluid velocity [m/s] ρ_f – Fluid density [kg/m^3] NTU – Number of Transfer Unit [-] L – Bed length [m] t – Time [s] ε – Bed porosity / Void fraction [-] ρ_s – Solid Density [kg/m^3] C_s – Solid specific heat capacity [J/kg-K] τ – Thermal time constant [-]

2.2. The E-NTU Model

The Hughes E-NTU model relies on a bed segment temperature approximation to formulate the numerical solution of discretized forms of the Schumann equations for the fluid and solid phases. The rock temperature is assumed to be constant in a given segment, while the air temperature has an exponential profile. One of the different numerical integration approaches may be used to solve the equations in Table 2. Duffie and Beckman make use of Euler-stepping (Hughes et al., 1976; Duffie, 2013).

Tab. 2: The E-NTU equations for the fluid and solid phases

The E-NTU Model	Remark
$T_{fm+1} = T_{fm} - (T_{fm} - T_{sm})\left(1 - e^{-NTU(\frac{\Delta z}{L})}\right)$ $\frac{dT_s}{dt} = \frac{L}{\Delta z}\frac{1}{\tau}(T_{fm} - T_{sm})\left(1 - e^{-NTU(\frac{\Delta z}{L})}\right)$	T_{fm+1} - The air temperature at the next segment m – Node number [-] Δz – Bed segment length [m]

2.3. The Infinite-NTU Model

The Hughes et al. Infinite-NTU model relies on the assumption that the fluid and solid phases are in local thermal equilibrium all over the packed bed due to the sufficiently high convective heat transfer between the phases. This reduces the model approximation to a single governing equation given in Table 3. The outlet bed temperature is the same as the exit air temperature. The inlet and outlet temperatures of the fluid (air) are considered boundary conditions. Simple discretization and numerical integration of this equation demand significantly lower computational effort in comparison to the E-NTU model (Hughes et al., 1976; Duffie, 2013).

In this regard, Duffie and Beckman state that for the appropriateness of employing the Infinite-NTU model, the Biot number (Bi) is evaluated according to a general correlation in Table 3. The Bi number is recommended to be less than 0.1. They also state that for long-term performance predictions of Infinite-NTU as those obtained by assuming a finite-NTU, values of NTU higher than 25 are recommended. They also noted that even for NTU values as low as 10, the infinite-NTU model should still provide reasonable long-term performance predictions (Hughes et al., 1976; Duffie, 2013).

Tab. 2: The E-NTU equations for the fluid and solid phases

The Infinite NTU Model	Remark
$\frac{dT_b}{dt} = -\frac{\dot{m}C_{pf}}{(1-\varepsilon)A_{cs}\rho_s C_s}\frac{\partial T}{\partial z}$ $T_{bm\,new} = T_{bm\,prev} - \frac{\Delta\theta L}{2\Delta z}\left(T_{bm\,prev} - T_{bm-1\,new}\right)$ $\Delta\theta = \frac{\Delta t}{\tau}$ $Bi = \frac{hR}{k}$ $h = \frac{h_v}{surface\ area\ of\ pebbles\ per\ unit\ volume}$ $R = \frac{D}{2}$	T_b – Bed Temperature [^{0}C or K] Δθ – Dimensionless time [-] Bi – Biot number [-] k – Thermal conductivity [W/m-K] h – Area heat transfer coefficient [W/m^2-K] R – Equivalent radius of pebble [m]

2.4. Case Study Design Specifications and Assumptions

A typical rock-bed TES (Figure 2) characterized by its 1.80 m length in flow direction and 14.8 m^2 cross-sectional area was evaluated as a case study (Duffie, 2013). The rock-bed TES was modeled considering ten segments at a distance of 0.18 m each.

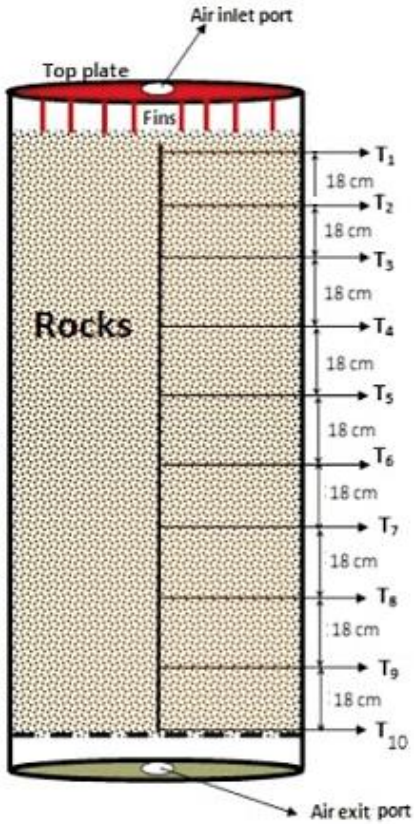

Fig. 2: A schematic of the rock bed system with the top (hot) plate installed, divided into sections for modeling

For the appropriateness and forecast study, properties of air and rock summarized in Table 4 and Table 5 were applied. All properties of air were evaluated at 20^0C since using a low temperature to evaluate air properties will be more severe for the evaluation of Bi and NTU criteria than if a high temperature. The bed was considered initially at 25^0C and the air inlet temperature is kept constant at 300^0C. To maintain a constant air temperature at the bed inlet, the mass flow rate of air through the open volumetric receiver, and hence the bed, must be modulated. In the Infinite-NTU simulations, the beds are treated as being perfectly insulated.

Tab. 4: Properties of Air

Parameter	Value
Velocity	0.053 m/s
Density	1.204 kg/m^3
Heat Capacity	1010 J/kg^{0}C

Tab. 5: Properties of rock

Parameter	Value
The equivalent diameter of the rock	12.5 mm
Density of rock	0.35
Void Fraction	1350 kg/m^3
Specific heat of rock	0.9 kJ/kg K
Thermal conductivity of rock	0.85w/m^{0}C
The surface area of rock per unit volume	255m^2/m^3

A non-zero mass flow rate should be detected when the bed enters charge mode with the charging airflow. Subsequently, the bed should enter discharge mode, with the discharging airflow temperature and mass flow rate. Discharging ceases once the air temperature at the bed outlet falls below the required limit, following which the bed may enter idle mode, remaining there until the next charge cycle begins (Figure 3).

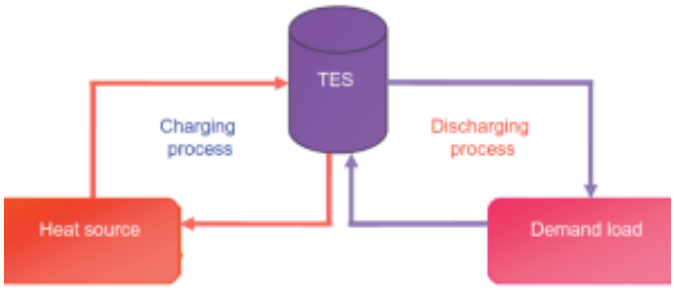

Fig. 3: Schematic of TES integration and operation

2.5. Infinite-NTU Prediction

There is an analytical solution for the Infinite-NTU prediction, but a numerical solution is generally more versatile. In the numerical solution of the Infinite-NTU equation, grid independence in both space and time should be demonstrated for discretization error to be minimized. For the rock-bed TES under consideration, the bed temperature was computed every hour at ten positions 0.18 m each from inlet to outlet. The Infinite-NTU model simulation was undertaken using the computational spreadsheet Excel.

3. Results and Discussion

3.1. The Bi number and NTU

Since the calculated Bi number (0.0587) is less than 0.1, the temperature gradient in the rock is not significant and thus E-NTU is nearly the same as Infinite-NTU. The NTU (68.15) is much larger than 10, this gives the same long-term performance predictions of the Infinite-NTU model essentially as those obtained by assuming a finite-NTU. Therefore, the Infinite-NTU model is found to be appropriate to predict the air outlet temperature and bed temperature at different nodes.

3.2. The Temperature Profiles

The convergence of the Infinite-NTU numerical solution for the charging operation is shown in Figure 4, which displays a very important attribute associated with the Infinite-NTU model. The figure illustrates the bed inlet starts charging in less than one hour. The number of hours that the bed operates in charging mode is around 22 hours.

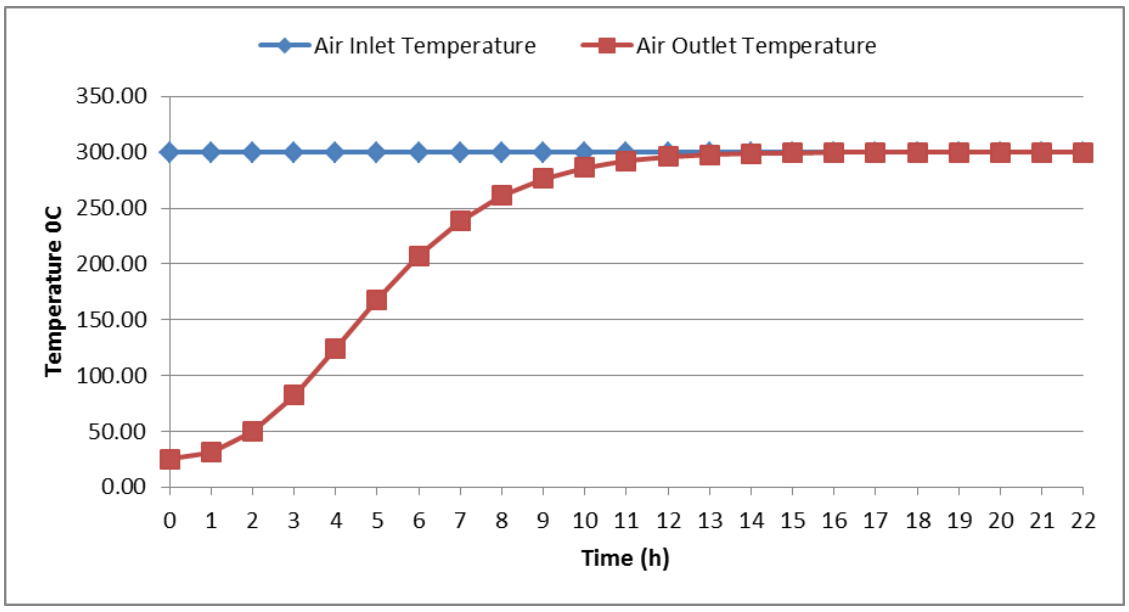

Fig. 4: Inlet and outlet air temperature for every hour operation

Figure 5 illustrates the lag between the bed inlet and outlet during charging operation. The number of hours that the bed lags to fully charge the bed outlet is around 12 hours from the fully charged bed inlet.

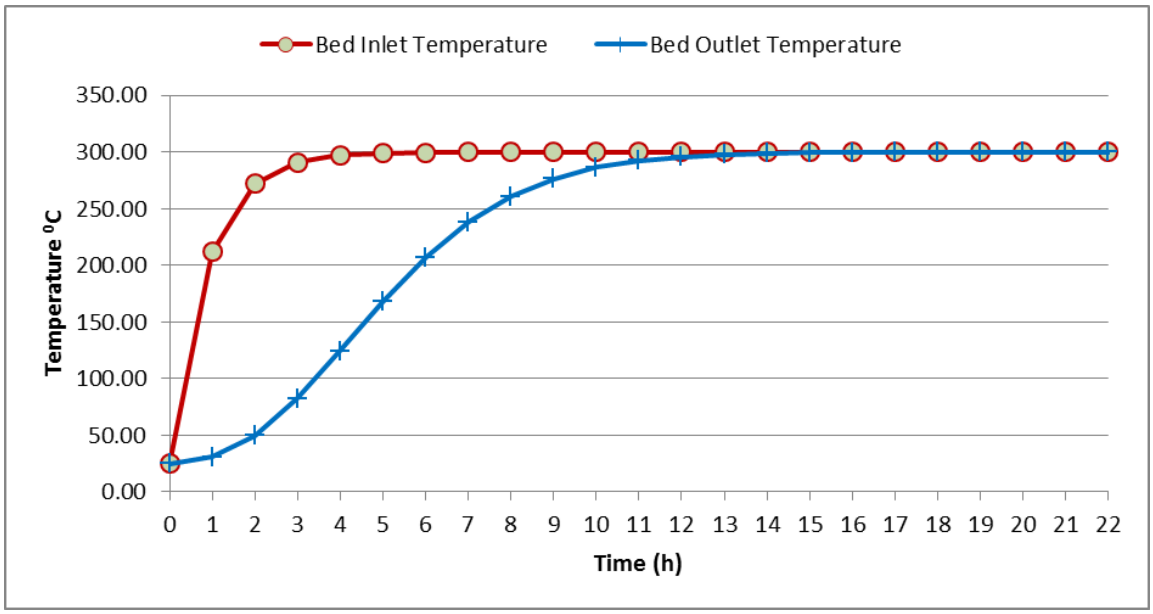

Fig. 5: Inlet and outlet bed temperature for every hour operation

Figure 6 appears to shows the ten nodes prediction of the Infinite-NTU numerical solution at every hour. The results also suggest the ten nodes achieve the inlet air temperature in 10, 12, 14, 15, 16, 17, 19, 20, 21, and 22 hours respectively. The charging rate is low when the change in temperature between the supply air and the bed segment becomes smaller.

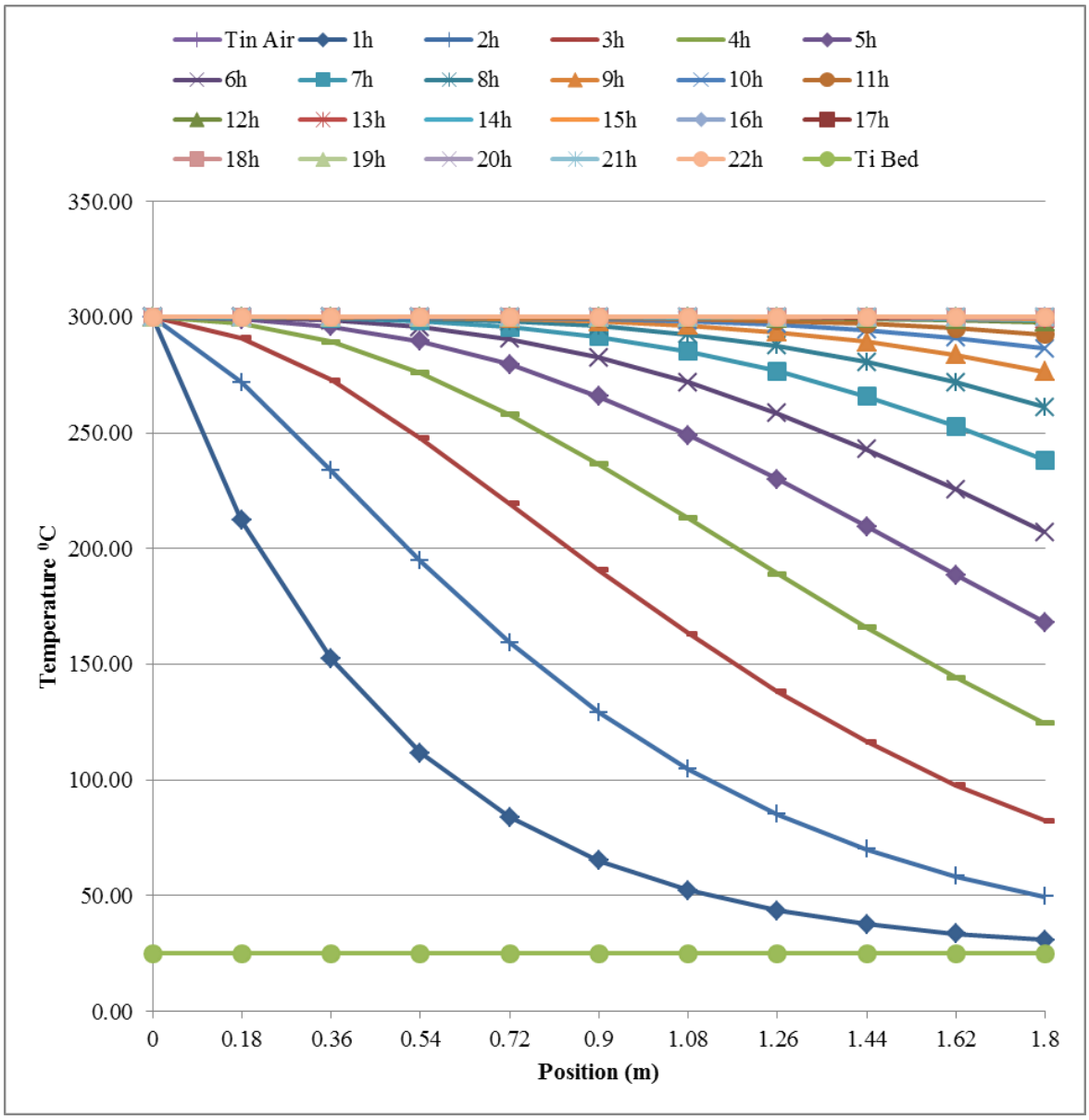

Fig. 6: Bed temperature prediction at the start and end of charging

4. Conclusions

Cost-effective packed-bed thermal containers filled with a solid storage medium have been proposed for sensible heat storage as materials are abundant and relatively cheap. Since it is essentially necessary to assess and predict their temperature profiles during the charge-discharge cycle, a time-efficient and less costly model is necessary. Thus, the simplified Infinite-NTU model is found to be very important. In this paper, the suitability of this less realistic model for a typical and scalable rock-bed TES using air as a charging medium was assessed first for the case study. With the given parameters, numerical solutions to this model were computed to obtain the temperatures of the air and the bed at different times and segments of the bed during charge cycles. The results suggest that the Infinite-NTU model can be appropriate in predicting the air and bed temperatures. The air outlet temperature exponentially reached the inlet temperature during the charging cycle operation. These predictions together with the material properties of the storage medium are very important to determine the design and operational characteristics as well as the performance of the rock-bed thermal energy storage system including the system power capacity, energy storage duration, and energy storage density. Such a reliable knowledge of the TES charge-discharge cycle temperature profile predictions is pre-conditions to plan, design, and rapidly deploy a reliable and economical solar thermal system for high-temperature applications of power generation and supply of valuable heat for high temperature demanding industrial processes like steel, brick, plastic, etc manufacturers. This is also very important to rapidly convert the use of fossil fuels to non-polluting renewable energy sources.

5. Acknowledgments

The author would like to acknowledge funding from CoE in REWiSE project at Mekelle University for the Ph.D. study leading to this article.

6. References

Duffie, J. A. and W. A. B. (2013). *Solar Engineering of Thermal Processes* (Fourth Edi). USA: John Wiley & Sons.

Furbo, S. (2015). Using water for heat storage in thermal energy storage (TES) systems. In Advances in Thermal Energy Storage Systems: Methods and Applications (pp. 31–47). Elsevier Inc. doi: 10.1533/9781782420965.1.31

Global Energy Systems Program. (2020). *Global Energy Storage Database | Energy Storage Systems*. U.S. Department Of Energy - DOE. Retrieved from https://www.sandia.gov/ess-ssl/global-energy-storage-database-home/

Heliodyne. Inc. (n.d.). *Heliodyne Commercial - Case Studies PDF Files*. Retrieved from http://www.heliodyne.com/commercial/case_studies/Lucky_Lab_press.pdf

Hoivik, N., Greiner, C., Tirado, E. B., Barragan, J., Bergan, P., Skeie, G., Blanco, P., & Calvet, N. (2017). Demonstration of EnergyNest thermal energy storage (TES) technology. *AIP Conference Proceedings*, *1850*(1), 80011. doi: 10.1063/1.4984432

Hughes, P. J., Klein, S. A., & Close, D. J. (1976). Packed bed thermal storage models for solar air heating and cooling systems. *ATJHT*, *98*, 336–338. Retrieved from https://ui.adsabs.harvard.edu/abs/1976ATJHT..98..336H/abstract

Jacob, R., Saman, W., & Bruno, F. (2017). Capital cost expenditure of high temperature latent and sensible thermal energy storage systems. *AIP Conference Proceedings*, *1850*. doi: 10.1063/1.4984433

Kolb, G. J., Ho, C. K., Mancini, T. R., & Gary, J. A. (2012). Power tower technology roadmap and cost reduction plan. In Concentrating Solar Power: Data and Directions for an Emerging Solar Technology (pp. 223–250). Retrieved from https://www.osti.gov/biblio/1011644

Kulkarni, G. N., Kedare, S. B., & Bandyopadhyay, S. (2008). Design of solar thermal systems utilizing pressurized hot water storage for industrial applications. *Solar Energy*, *82*(8), 686–699. doi: 10.1016/j.solener.2008.02.011

Kuravi, S., Trahan, J., Goswami, D. Y., Rahman, M. M., & Stefanakos, E. K. (2013). Thermal energy storage technologies and systems for concentrating solar power plants. In Progress in Energy and Combustion Science (Vol. 39, Issue 4, pp. 285–319). Pergamon. doi: 10.1016/j.pecs.2013.02.001

McTigue, J. D., & White, A. J. (2018). A comparison of radial-flow and axial-flow packed beds for thermal energy storage. *Applied Energy*, *227*, 533–541. doi: 10.1016/j.apenergy.2017.08.179

Schumann, T. E. W. (1929). Heat transfer: A liquid flowing through a porous prism. *Journal of the Franklin Institute*, *208*(3), 405–416. doi: 10.1016/S0016-0032(29)91186-8

Wakao, N., Kaguei, S., & Funazkri, T. (1979). Effect of fluid dispersion coefficients on particle-to-fluid heat transfer coefficients in packed beds. Correlation of nusselt numbers. *Chemical Engineering Science*, *34*(3), 325–336. doi: 10.1016/0009-2509(79)85064-2

Wallerand, A. S., Kermani, M., Voillat, R., Kantor, I., & Maréchal, F. (2018). Optimal design of solar-assisted industrial processes considering heat pumping: Case study of a dairy. *Renewable Energy*, *128*, 565–585. doi: 10.1016/j.renene.2017.07.027

Zanganeh, G., Pedretti, A., Zavattoni, S., Barbato, M., & Steinfeld, A. (2012). Packed-bed thermal storage for concentrated solar power - Pilot-scale demonstration and industrial-scale design. *Solar Energy*, *86*(10), 3084–3098. doi: 10.1016/j.solener.2012.07.019

Zhang, H., Baeyens, J., Cáceres, G., Degrève, J., & Lv, Y. (2016). Thermal energy storage: Recent developments and practical aspects. In Progress in Energy and Combustion Science (Vol. 53, pp. 1–40). Elsevier Ltd. doi: 10.1016/j.pecs.2015.10.003